

# EXPERIMENTAL STUDY OF EXCITED CIRCULAR CYLINDER IN CURRENT

**Kyrre Vikestad**

Department of Marine Structures  
Norwegian University of Science and Technology  
Trondheim, Norway

**Carl M. Larsen**

Department of Marine Structures  
Norwegian University of Science and Technology  
Trondheim, Norway

**J. Kim Vandiver**

Department of Ocean Engineering  
Massachusetts Institute of Technology  
Cambridge, Massachusetts

## ABSTRACT

This paper presents results from experiments with an elastically supported cylinder subjected to support motions and fluid flow. We varied the support motion amplitude, frequency and flow velocity. We show how this external disturbance influence on the vortex shedding frequency, cylinder oscillation amplitude at the vortex shedding frequency and at the support oscillation frequency. Energy dissipation from the cylinder into the fluid is given in terms of the transverse drag coefficient  $C_d$ . Results show that the external disturbance has limited influence on the vortex shedding frequency, except for the case where the vortex shedding frequency coincide with the support frequency. Response from support motion tends to be more damped in fluid flow than in still water. Response at the vortex shedding frequency is reduced by the external disturbance, if the disturbance frequency is different from the vortex shedding response frequency.

## NOMENCLATURE

$A$	equivalent cylinder motion amplitude at a given frequency
$C_a$	added mass coefficient
$C_d$	drag coefficient for the cross-flow motion
$D$	test cylinder diameter (10.0 cm)
$F_v$	vertical component of hydrodynamic force
$f_e$	support motion frequency in Hz
$f_0, f_{dry}$	natural frequencies, still water and air
$KC$	Keulegan-Carpenter no. for oscill. flow = $\frac{U_{max}}{fD}$
$L$	length of test cylinder (2.0 m)
$Re$	Reynolds number = $\frac{UD}{\nu}$
$U$	current flow velocity
$U_r$	reduced velocity = $\frac{U}{Df_0}$
$y_0$	support motion amplitude
$\beta$	viscous-frequency parameter = $\frac{Re}{KC} = \frac{D^2}{\nu T}$

## INTRODUCTION

Long marine risers subjected to current may due to vortex shedding have an oscillating motion in the cross flow direction. A broad discussion of this phenomenon is given by Vandiver (1993), where the experience from several experiments is used to explain the significance of the dimensionless parameters that often are applied to characterize a particular case. The flow excitation, or damping, along the riser is dependent on various parameters such as the reduced velocity  $U_r$ , the Reynolds number  $Re$  and the riser motion at the given location. The local riser motion is in turn a function of the fluid forces over the entire riser. Due to variation in the current velocity and cross section motion along the riser, excitation frequencies may also vary. If so, there must be some kind of interaction between these frequencies. Such interaction must be fully understood in order to establish a mathematical model for multi-frequency response. Two aspects of interaction are important:

**Excitation zones:** It is not straightforward to identify excitation zones along the riser for each possible frequency simply because single-frequency models will predict a zone for one frequency that easily will overlap with another. As the vortex shedding process at one specific position along the riser cannot consist of two independent processes with different frequencies, a strategy for elimination of zone overlaps must be established.

**Damping/excitation interaction:** In a zone with excitation on one frequency, the riser will also feel a response at another frequency due to excitation on a neighboring zone. Two questions arise:

- how will the response at one frequency influence the excitation at another frequency?
- how can damping at one frequency be modeled in a zone where excitation at another frequency takes place ?

Stiffness of lower spring	$k_1$	503.4	N/m
Stiffness of upper spring	$k_2$	467.5	N/m
Tot. stiffn. incl. water plane,	$k_{tot}$	998.9	N/m
Cylinder volume	$V_{cyl}$	.0157	$m^3$
Nat. freq. in air,	$f_{dry}$	.9815	Hz
Nat. freq. in still water,	$f_0$	.79	Hz
Effective dry mass	$m$	25.53	kg
Effective wet mass		40.54	kg
$C_a$ at $f_0$		.956	
Mass ratio (dry mass/ $\rho D^2 L$ )		1.277	
Specific gravity (dry mass/displ. water)		1.625	
Relative damping in air		.147	%

Table 1: The properties of the apparatus

Commonly applied models for prediction of vortex induced vibrations do not have a good description of these effects, and such models will therefore be associated to a significant uncertainty as shown by Larsen and Halse (1995). In order to investigate this problem, a new type of experiment with an oscillating cylinder in current has been carried out at the hydrodynamic laboratories in Trondheim. In these tests the cylinder was simultaneously excited by vortex shedding and spring support motions. The change of pipe behavior from a single-action to a double-action test can hence be identified, and thereby a model for interaction between excitation and damping be established. It is also possible to investigate how the response from the spring support excitation - regarded as a disturbance - will influence the vortex shedding frequency, which is the key to understand how excitation zones will develop along a riser.

## EXPERIMENT SETUP AND INSTRUMENTATION

The apparatus designed for the present experiments is shown in Fig. 1. An early report from the experiment is given by Larsen et al. (1996). The test cylinder is supported by two springs. The end of one spring is linked to a mechanism that provide harmonic vertical motions with a wanted amplitude and frequency. Both ends of the cylinder (position A on the figure) were equipped with load cells making it possible to measure horizontal and vertical force components. The hydrodynamic force (pressure resultant on the cylinder) can easily be found by subtracting the dry inertia force from the measured, and further processing will give drag, lift and added mass. At the excitation mechanism (position B) acceleration and spring force were measured. It is hence possible to calculate the amount of energy transmitted from the excitation mechanism to the cylinder. Finally, vertical accelerations of the cylinder were recorded at the top of the vertical bars in the frame (position C). A position meter was also installed to ensure that the exact displacement could be found. In total 12 channels were applied, all working at a sampling frequency of 60 Hz. The apparatus was installed on the carriage in a small towing tank and towed at the wanted speed in order to simulate constant current with low turbulence. The length of the cylinder is 2 m and the diameter is 0.1 m. Thin plates were mounted on both ends in order to reduce any end effects and influence from the sides of the towing tank. Reynolds

number for these experiments was always in the sub-critical regime, ranging from approximately 15,000 to 120,000. Key data for the apparatus are given in Table 1.

Efforts has been made in order to keep the apparatus a single degree of freedom system with low damping in air. The natural frequency for the pitch mode was approximate 2.5 Hz, which is well apart from the vertical mode. Disturbance from pitch motions was never observed.

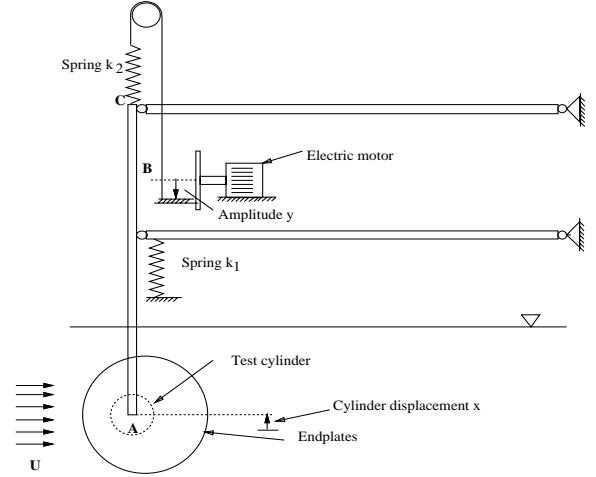


Figure 1: The apparatus

## Experimental Matrix

Still water oscillation tests were done in order to verify the apparatus and give a basis for comparison for the towed cases. The apparatus was excited with several motor frequencies  $f_e$  and amplitudes ( $y_0$ ).

Tow without excitation were conducted for reduced velocities from 3.5 to 13. The frequency used in the definition of  $U_r$  is the natural frequency in *still water*.

Tests combining different  $U_r$ ,  $f_e$  and  $y_0$ : 9 different reduced velocities (3.3 — 8.5), 14 different frequencies ( $f/f_0$  from .57 to 2.40) and 5 different amplitudes (1, 2, 3, 5 and 7 cm). The length of each tow was approximate 18 meters.

## MATHEMATICAL DESCRIPTION

The system can be described by the dynamic equilibrium equation:

$$m\ddot{x} + c\dot{x} + k_{tot}x = F_v(t) + k_2y(t) \quad (1)$$

where  $m$  is the dry mass of the cylinder,  $c$  the structural damping coefficient found from decay test in air.  $F_v$  is the vertical component of the hydrodynamic force,  $x$  is the cylinder motion and  $y$  is the motion of the excitation system. If the response is assumed to be harmonic  $x(t) = x_0 \sin(\omega t)$ , we may assume that  $F_v = F_0 \sin(\omega t + \phi)$ . Using the know properties

$$F_0 \sin(\omega t + \phi) = F_0 \cos(\phi) \sin(\omega t) + F_0 \sin(\phi) \cos(\omega t) \quad (2)$$

we can split the fluid force into parts proportional to the cylinder acceleration and velocity:

$$\left(m + \frac{F_0 \cos(\phi)}{\omega^2 x_0}\right) \ddot{x} + \left(c - \frac{F_0 \sin(\phi)}{\omega x_0}\right) \dot{x} + k_{tot} x = k_2 y(t) \quad (3)$$

Using that

$$\lim_{T \rightarrow \infty} \frac{\int_t^{t+T} F_v \cdot \dot{x} dt}{T} = \frac{1}{2} \omega x_0 F_0 \sin(\phi) \quad (4)$$

and

$$\lim_{T \rightarrow \infty} \frac{\int_t^{t+T} F_v \cdot \ddot{x} dt}{T} = -\frac{1}{2} \omega x_0^2 F_0 \cos(\phi) \quad (5)$$

equation 3 can be written

$$\left(m - \frac{\lim_{T \rightarrow \infty} \frac{2 \int_t^{t+T} F_v \cdot \ddot{x} dt}{(\omega^2 x_0)^2}}{\right) \ddot{x} + \left(c - \frac{\lim_{T \rightarrow \infty} \frac{2 \int_t^{t+T} F_v \cdot \dot{x} dt}{(\omega x_0)^2}}{\right) \dot{x} + k_{tot} x = k_2 y(t) \quad (6)$$

A good approximation for the limits shown above is found by integrating over an integer number of oscillation periods. We can now find the added mass and transverse drag coefficients,  $C_a$  and  $C_d$  from

$$C_a = -\frac{\lim_{T \rightarrow \infty} \frac{\int_t^{t+T} F_v \cdot \ddot{x} dt}{T}}{\rho \pi \frac{D^2}{8} L (\omega x_0)^2} \quad (7)$$

$$C_d = -\frac{\lim_{T \rightarrow \infty} \frac{\int_t^{t+T} F_v \cdot \dot{x} dt}{T}}{\rho L D \frac{2}{3\pi} (\omega x_0)^3} \quad (8)$$

The drag coefficient corresponds to the one that gives a correct loss of energy per cycle using Morison's equation (Morison et al. (1950)) for a single peak response spectrum. It is in principle the same as applied by Keulegan and Carpenter (1958). If the response spectrum has more than one peak, the usefulness of the coefficients will depend on the relative magnitude of the peaks.

### Harmonic Excitation And Current

Under combined action from support excitation and vortex shedding from current, the cylinder will no longer respond at a single frequency but may have both support and vortex shedding frequencies in the motion. If these two frequencies are well apart, it is possible to separate the response spectrum into one "support motion domain" and one "vortex shedding domain". In order to interpret the measurements in an approximate way, the response spectrum in these two domains are used to define an "equivalent response amplitude" from the well-known relation

$$\frac{1}{2} A^2 = \int_{\Delta\omega} S_x(\omega) d\omega \quad (9)$$

where  $A$  is an equivalent response amplitude for the peak located in the  $\Delta\omega$  frequency domain.  $S_x(\omega)$  is the response

spectrum. If the integral is taken over the vortex shedding domain,  $A$  is considered to be an amplitude caused by vortex shedding, while the support motion domain will give the amplitude caused by support motion. This definition of  $A$  means that  $A$  represents an equivalent amplitude, in contrast to the root mean square value (rms). The ratios between equivalent amplitudes and amplitudes found from single-action tests can be applied to characterize the influence from a disturbance on vortex shedding excitation, and also the influence from vortex shedding at one frequency on damping of motions at another frequency.

## RESULTS AND DISCUSSION

### Still Water Oscillation Test

Putting the cylinder in water reduced the natural frequency considerably. An approximation for the natural frequency in water was found by exciting with small support amplitude for different frequencies, and then find the frequency for maximum response. The reduction of the natural frequency indicates an added mass coefficient of  $C_a = 0.956$ . In Fig. 2(b), which is computed from the experiment, the added mass coefficient is found to be approximate 1.0 for small amplitudes, consistent with potential theory. The drag coefficient plot in Fig. 2(a) shows a minimum  $C_d$  value of approximate 0.5 at non-dimensional amplitude  $A/D = 0.3$ . For low amplitude values skin friction becomes significant and  $C_d$  is proportional to  $(A/D)^{-1}$  according to Stokes law. In the present experiment, the curve for 0.86 Hz ( $\beta = 11600$ ) seems to fit very well with the log-log plot for  $\beta = 11240$  given by Sarpkaya (1986). Both the minimum value and the value for  $KC \approx 9$  correspond. For small amplitudes, the numerical values are very sensitive to errors in force and velocity.

### Flow Without External Excitation

Results from the towed cylinder tests are shown in Fig. 3. Here the cylinder response was limited to a narrow frequency band, and Eq. 7 can be applied for calculation of the added mass. Fig. 3(a) shows that added mass varies considerably and becomes negative for high reduced velocities. In Fig. 3(b) the ratio between the oscillation frequency and the "true natural frequency"  $f_{nat}$  where the added mass is included, is approximate unity for all tested reduced velocities. The "true natural frequency" is found from

$$f_{nat} = \frac{1}{2\pi} \sqrt{\frac{k_{tot}}{m + C_a(U_r) \rho V_{cyl}}} \quad (10)$$

where  $C_a$  is a function of the reduced velocity  $U_r$ . The tendency is that the added mass adapt to a value giving oscillations at a resonant frequency. Using  $f_{nat}$  instead of  $f_0$  in the definition of  $U_r$  will in this case correspond to the "true reduced velocity" given by Moe and Wu (1989). The curves are seen to exhibit a less consistent trend for reduced velocities above 10.

### Flow And Support Excitation

The support excitation will influence cylinder motions and thereby the vortex shedding process behind the cylinder. The time-averaged power put into the system from the support motion,  $W_{s,m}$ , can be divided into structural damping,

$W_{str}$ , and fluid damping,  $W_{fluid}$ , as shown in Eq. 11. Since the structural damping is very low, the time-averaged power balance is a matter of power from the motor to the fluid, or from the fluid to the motor.

$$W_{s.m} + W_{fluid} + W_{str} = 0 \quad (11)$$

Fig. 4 shows the regions where the peak vortex shedding frequency  $f_v$  coincides with the support excitation frequency  $f_e$ . Be aware of the limited  $U_r$  in this experiment. For the free oscillation curve, the peak oscillation frequency  $f_v$  is used instead of the support excitation frequency  $f_e$ . From the rather narrow band in Fig. 4(a) to the broad band in Fig. 4(d) we may see the effect of increasing support amplitude. It appears that for a given support excitation frequency, the upper limit in  $U_r$  corresponds to the reduced velocity for a free cylinder, oscillating at the same frequency. This may be due to the fact that the fluid force is mainly proportional to the square of the  $U_r$  and therefore often will be the dominating force for high  $U_r$ .

The results from combined support and current excitation can be divided into three main areas dependent on the support excitation frequency:

1. low frequency: 0.45, 0.52 and 0.58 Hz
2. frequency in the still water natural frequency region: 0.75, 0.78, 0.81 and 0.85 Hz
3. high frequency: 1.11, 1.36, 1.64 and 1.90 Hz

By grouping the results this way, we can describe what characterizes each group.

**Low Support Frequency.** When the support frequency is low, the energy associated with oscillations at the frequency is low compared to oscillations at the natural frequency. In the experiment, still water oscillation amplitudes due to support excitation is in the range 0.07 — 0.68 A/D. One may therefore assume that a disturbance at this frequency has only a moderate influence on the vortex shedding forces at reduced velocities in the lock-in regime and above. The result for 0.52 Hz is shown in Fig. 5. Fig. 5(a) shows the oscillation frequency due to vortex shedding. For high support oscillation amplitudes and  $U_r \approx 3-4$  the frequency is locked on to the support frequency. Otherwise, the frequency appears slightly higher than for the undisturbed oscillation case. This pattern is common for all support excitation frequencies. There can be two explanations:

1. The free oscillation frequency found from one test for each reduced velocity is not representative for free oscillations. Several tests should have been conducted and a mean value identified
2. The disturbance of the wake due to support oscillation increases the shedding frequency.

One can also see that if the vortex shedding frequency is different from the support frequency, the frequency of the vortex shedding response is in general not very dependent on the support motion. The amplitude at 0.52 Hz shown in Fig. 5(b) is close to the still water amplitude. The still water amplitudes for different support amplitudes are given in the figure legend. One can see that the amplitudes in general decrease for increasing  $U_r$ . The same tendency is also seen for the 0.45 and 0.58 Hz cases. For low  $U_r$  it was impossible to distinguish between response at the support frequency and at the vortex shedding frequency. The response amplitude

at the support frequency was then defined to be zero and the total response regarded as a vortex induced response.

The magnitude of the transverse “drag coefficient”  $C_d$  given in Fig. 5(c) is not very interesting, since there are two different oscillation frequencies involved. This coefficient is found using Eq. 8 where  $\omega x_0$  is set to be  $\sqrt{(vel_{freq1})^2 + (vel_{freq2})^2}$ . A positive  $C_d$  means that the fluid forces in total are damping, and that the support motions are exciting. It will not describe any possible energy transport between the frequencies. The characteristic behavior of the  $C_d$  for low frequency support oscillation is as follows:

- positive  $C_d$  of the same order as still water  $C_d$  may be assumed for very low  $U_r$
- $U_r = 4-5$ : drop in the drag coefficient to a negative value. From the 0.45 Hz and 0.58 Hz results, it appears that the  $U_r$  level where  $C_d$  turns positive increases with increasing support frequency.
- for  $U_r \approx 5$  the  $C_d$  declines towards zero or negative values for  $U_r \approx 7$ . There is a clear connection between higher support amplitude and higher  $C_d$ . The denominator in Eq. 8 is in this  $U_r$  region fairly constant, meaning that  $C_d$  is a measure for the relative energy dissipation for different amplitudes.
- for  $U_r$  greater than 7,  $C_d$  is mostly negative, and no obvious relation between the amplitudes is seen.

Fig. 5(d) shows the support excitation influence on the cylinder amplitude at the vortex shedding frequency. The maximum amplitude is reduced, and the lock-in region has become more narrow. In the lock-in region, we can see that increasing support amplitude will reduce the vortex induced vibration (VIV) amplitude.

### Support Frequency Near Still Water Natural Frequency

**0.79 Hz.** The result for 0.81 Hz is shown in Fig. 6. Now the still water amplitude is near its maximum due to resonance. Maximum cylinder amplitude for 7 cm support amplitude is 1.35 A/D. The support excitation is now so powerful that it fully controls the vortex shedding frequency over a wide range of reduced velocities as seen in Fig. 6(a). From both Fig. 6(a) and Fig. 4 we can see that the reduced velocity for an undisturbed cylinder, oscillating with the support frequency, is an upper limit for frequency synchronization. The reduction of amplitude at the support frequency is clearly seen in Fig. 6(b), even though it is given only for high and low  $U_r$ . Plots for other support frequencies near 0.79 Hz confirm that the amplitude is reduced to approximate half the still water amplitude. The reduction is seen to be larger for high  $U_r$  than for low.

The transverse drag coefficient  $C_d$  (Fig. 6(c)) now behaves as for low support frequencies, with the main difference that the drop to negative  $C_d$  for  $U_r = 4-5$  has disappeared. For high  $U_r$ , large support amplitudes will mainly give positive drag, while negative drag is found for smaller amplitudes. Amplitude at the vortex shedding frequency is shown in Fig. 6(d). For  $U_r \approx 3.3$ , the vortex shedding for 1 and 2 cm support amplitude is at a frequency corresponding to a free cylinder, while higher support amplitudes give frequency synchronization. For the 3 cm support amplitude case, the VIV amplitudes are reduced compared to still water amplitudes, whereas for 5 and 7 cm the VIV amplitudes have increased. This pattern is also seen for the other support frequencies near 0.79 Hz. This may indicate that the

ability to control the vortex shedding process may be present before the ability to extract energy from the wake. Except for the low  $U_r$  amplitudes dominated by the near resonance support motion, VIV amplitudes are reduced compared to free cylinder motions. Even for the  $U_r \approx 5.8$  where the free oscillation frequency corresponds to the support frequency, the VIV amplitude is not increased. Common for all support frequencies near 0.79 Hz is that one  $U_r$  can be found where the VIV amplitude curves seem to more or less fall into the same  $U_r - A/D$  point, and that the A/D curve for free cylinder also goes through that point, cf. 6(d).

**High support frequency.** The result for 1.36 Hz is shown in Fig. 7. Now the VIV frequency for the given  $U_r$  is not able to coincide with the frequency of the support motion. But we can observe a coupling between the VIV frequency and one third of the support frequency. (See Williamson and Roshko (1988) for more on vortex formation.) This is seen in Fig. 7(a) for  $U_r = 3.3 - 4.1$  and 5 and 7 cm support amplitude. The same effect was seen for the 1.64 Hz case. In general, the vortex shedding frequency observed for cases with high frequent support motions seems to be insignificantly influenced by varying support amplitudes. Oscillation at the support frequency 1.36 Hz (Fig. 7(b)) is smaller than the still water amplitude for  $U_r = 5 - 6$ , except for the 1 cm support amplitude. The amplitude is increasing with increasing  $U_r$ . In the 1.64 and 1.90 Hz tests, reduced velocity variations had very limited influence on the support frequency amplitudes. For the 1.11 Hz test the amplitudes increase with increasing  $U_r$ .

Oscillation amplitudes at the VIV frequency (Fig. 7(d)) are reduced by the support oscillation. It seems clear that increased support amplitudes will decrease the VIV amplitudes in the typical lock-in region. When increasing the support frequency from 1.11 Hz to 1.90 Hz, both the still water amplitudes and the effect on the VIV amplitudes are reduced.

## CONCLUSIONS

From the discussion above, the following conclusions may be drawn:

- When there is no frequency synchronization, variation in vortex shedding frequency due to support excitation is limited
- Synchronization between support excitation and vortex shedding is strongly dependent on the size of the external disturbance and the reduced velocity
- Response due to support excitation far from the vortex shedding frequency is in general more damped when towed than in still water
- The response at the vortex shedding frequency is in general reduced due to support excitation

## Further Work

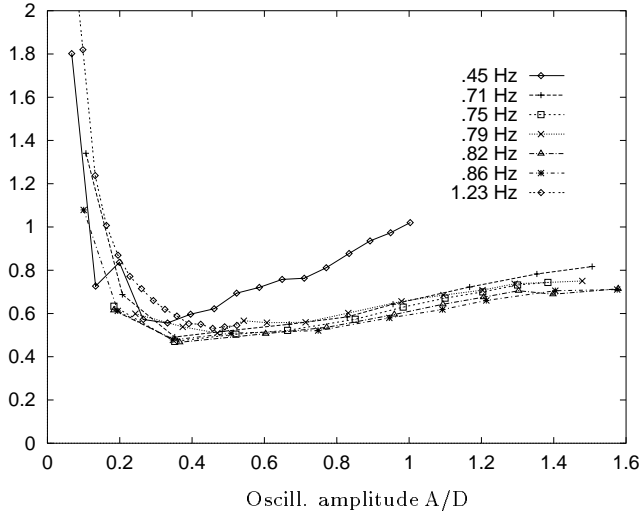
The experiments should be carried out for a wider range of reduced velocities. In the present investigation, due to variations in the in-line drag force, it was difficult to keep a constant tow velocity when towing at high velocities. Variations could be up to 10 %, and the results given in this paper for high  $U_r$  may not be of high quality. New experiments with an improved towing device should be carried out.

## ACKNOWLEDGMENT

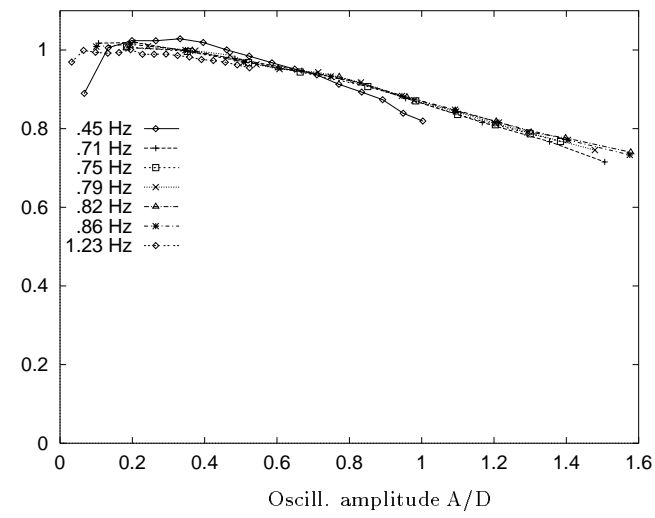
The experiments described in this paper have been financed by grants from the "Growth Point Centre on Hydro elasticity" at the Norwegian University of Science and Technology (NTNU). The authors wish to express their gratitude to SINTEF and NTNU who established and supported the Growth Point Centre and thereby made these experiments possible. Vandiver's participation was in part supported by the Office of Naval Research. The authors acknowledge Mr. A. Skagen of MARINTEK for skillful design of the apparatus, Mr R. Moe of NTNU for precise construction and Mr. T. Leer of NTNU for calibration of the apparatus.

## REFERENCES

- KEULEGAN, G. H. AND L. H. CARPENTER (1958). Forces on cylinders and plates in an oscillating fluid. *J. of Res. of the National Bureau of Standards* 60(5), 423-440.
- LARSEN, C. M. AND K. H. HALSE (1995). Comparison of models for vortex induced vibrations of slender marine structures. In *Proceedings of the Sixth International Conference on Flow-Induced Vibrations*, London UK, pp. 467-482.
- LARSEN, C. M., K. VIKESTAD, AND J. K. VANDIVER (1996). On multi-frequency vortex induced vibrations of long marine risers. In *Proceedings of Oceans 96 MTS/IEEE Conference*, Ft. Lauderdale, Florida.
- MOE, G. AND Z.-J. WU (1989, March 19-23). The lift force on a vibrating cylinder in a current. In *Eight International Conference on Offshore Mechanics and Arctic Engineering*, The Hague, The Netherlands, pp. 259-268.
- MORISON, J., M. O'BRIEN, J. JOHNSON, AND S. SCHAAF (1950). The force exerted by surface waves on piles. *Pet. Trans, AIME* 189, 149-154.
- SARPKAYA, T. (1986). Force on a circular cylinder in viscous oscillatory flow at low Keulegan-Carpenter numbers. *J. of Fluid Mechanics* 165, 61-71.
- VANDIVER, J. K. (1993). Dimensionless parameters important to the prediction of vortex-induced vibration of long, flexible cylinders in ocean currents. *J. of Fluids and Structures* 7, 423-455.
- WILLIAMSON, C. H. K. AND A. ROSHKO (1988). Vortex formation in the wake of an oscillating cylinder. *J. of Fluids and Structures* 2, 355-381.

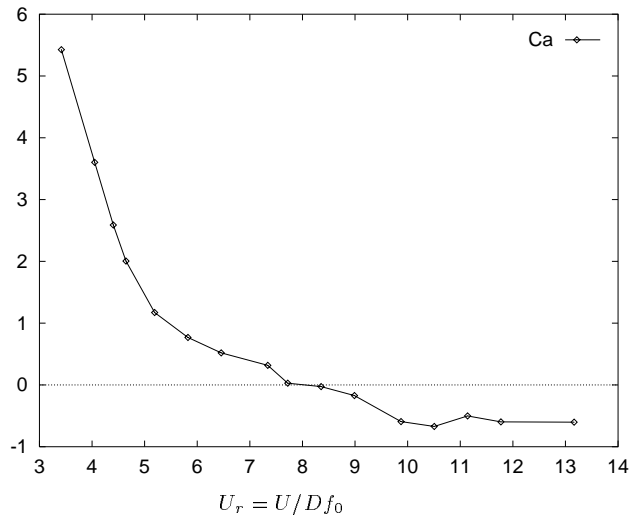


(a) Drag coefficient as a function of cylinder oscillation amplitude, frequency varied

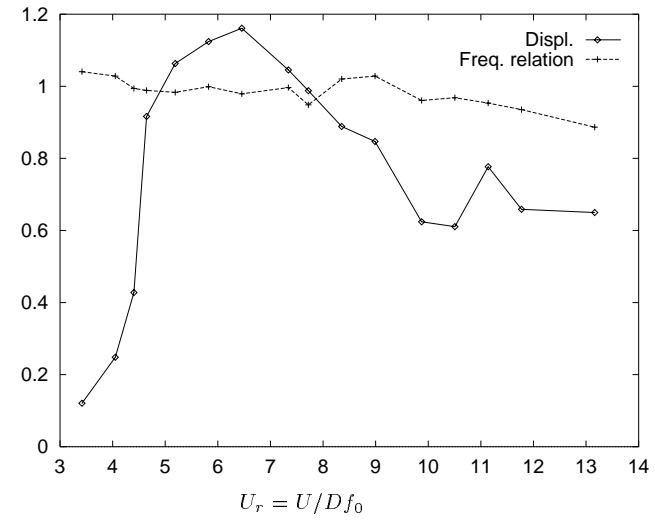


(b) Added mass coefficient as a function of cylinder oscillation amplitude, frequency varied

Figure 2: Cylinder oscillation in still water

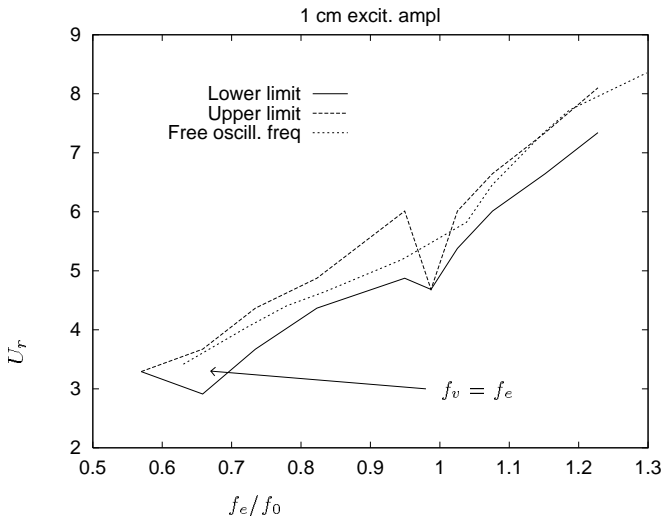


(a) Added mass coefficient as a function of reduced velocity

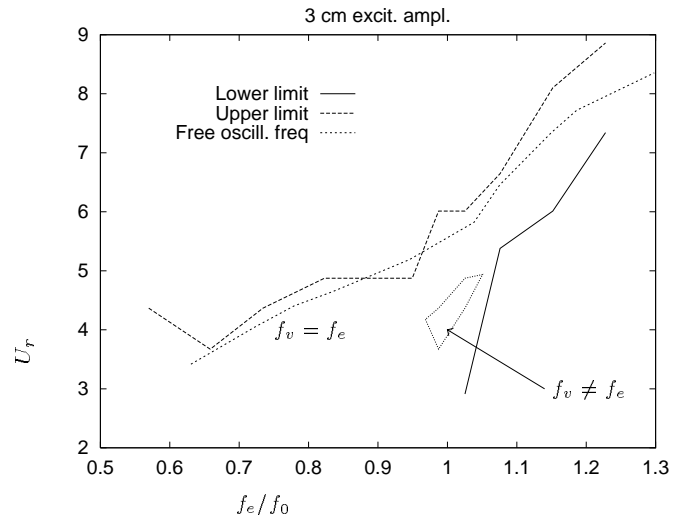


(b) Oscillation amplitude,  $A/D$ , and frequency ratio,  $f_{oscill}/f_{nat}$  as functions of reduced velocity

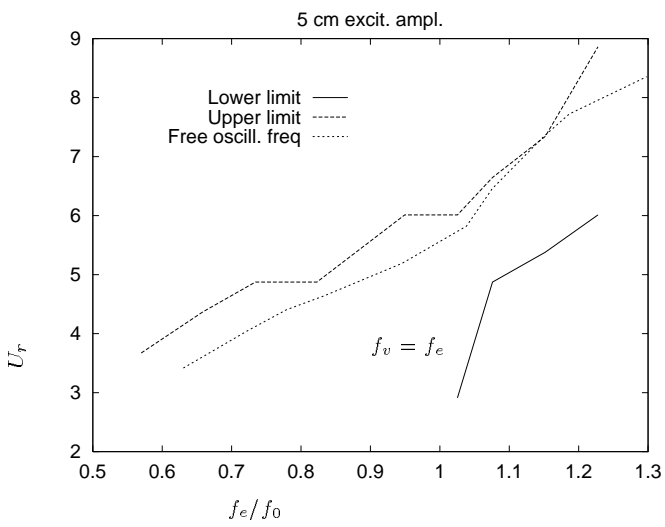
Figure 3: Towing without support oscillation; free oscillation



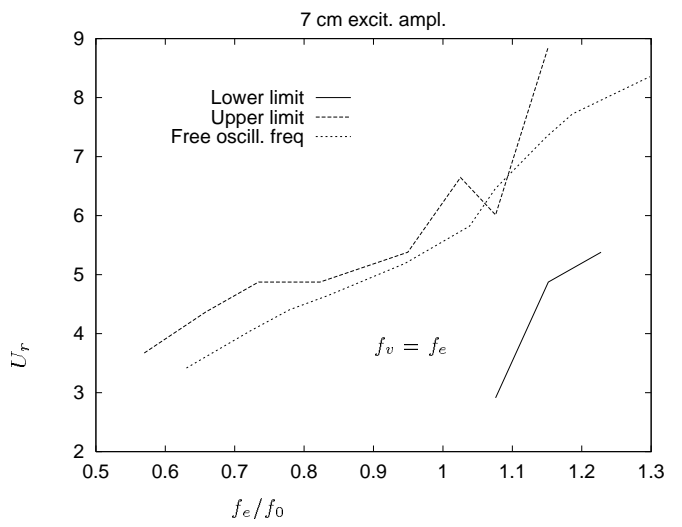
(a) Area where the peak vortex shedding frequency coincides with support oscillation frequency, 1 cm support amplitude



(b) Area where the peak vortex shedding frequency coincides with support oscillation frequency, 3 cm support amplitude

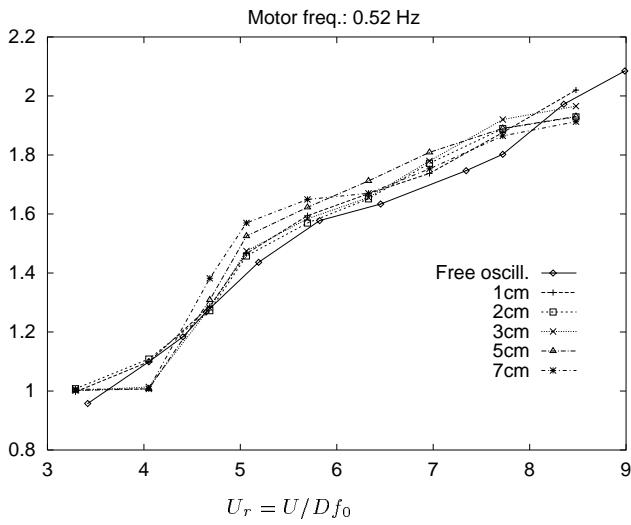


(c) Area where the peak vortex shedding frequency coincides with support oscillation frequency, 5 cm support amplitude

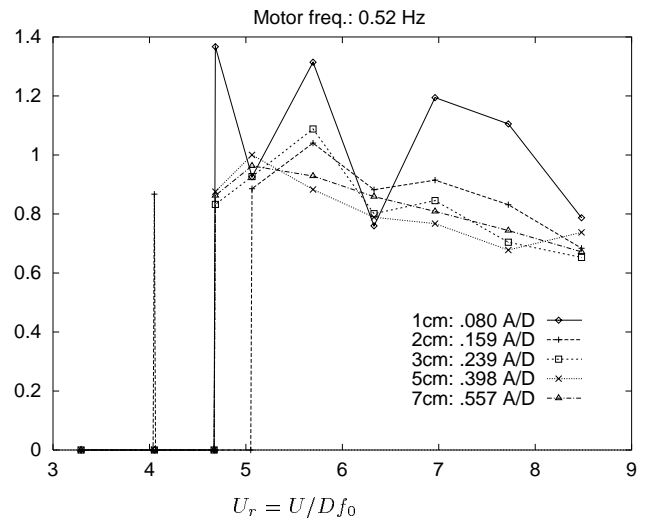


(d) Area where the peak vortex shedding frequency coincides with support oscillation frequency, 7 cm support amplitude

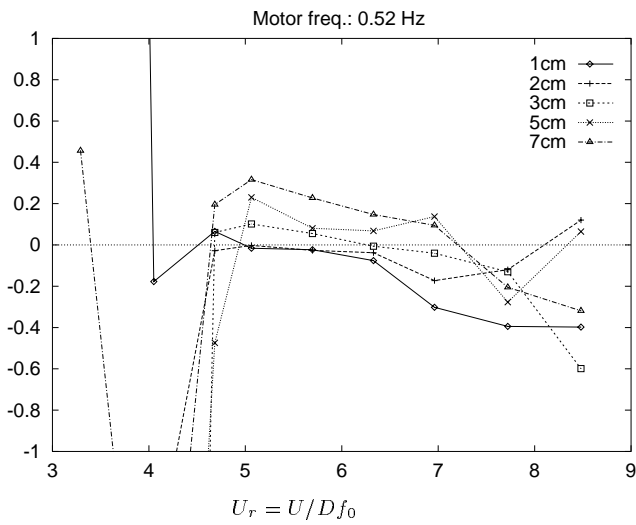
Figure 4: Peak vortex shedding frequency locked on to the support excitation frequency



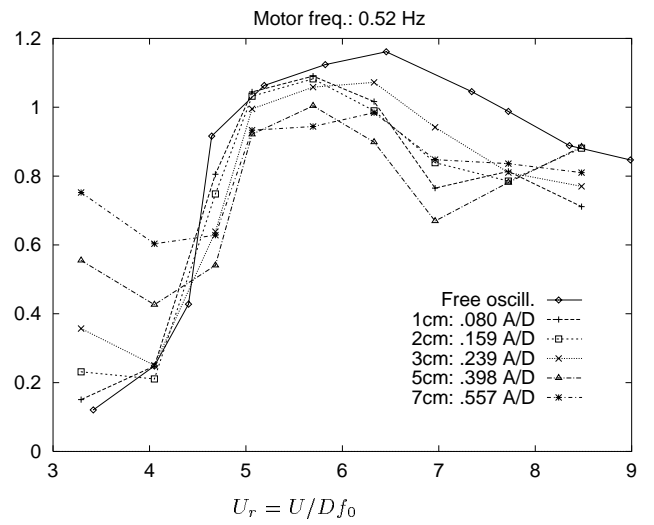
(a) Oscillation frequency due to vortex shedding over support excitation frequency



(b) Oscillation amplitude, A/D, at the support frequency, towed case, over oscillation amplitude in still water. The still water amplitude is found in the legend

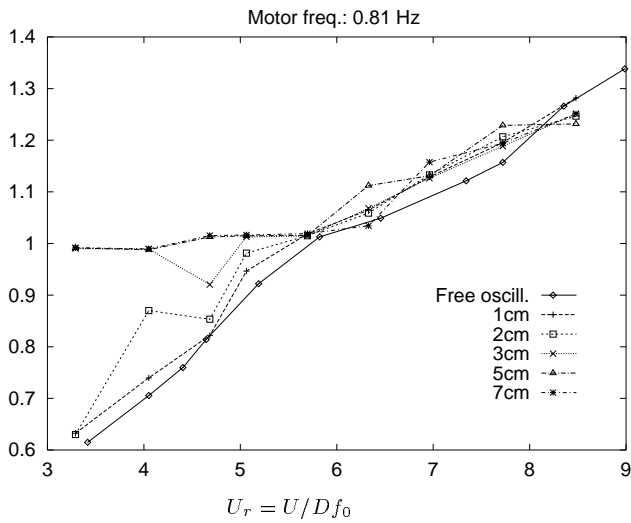


(c) Transverse "Drag coefficient"  $C_d$ : Positive coefficient denotes that the fluid forces take energy away from the system

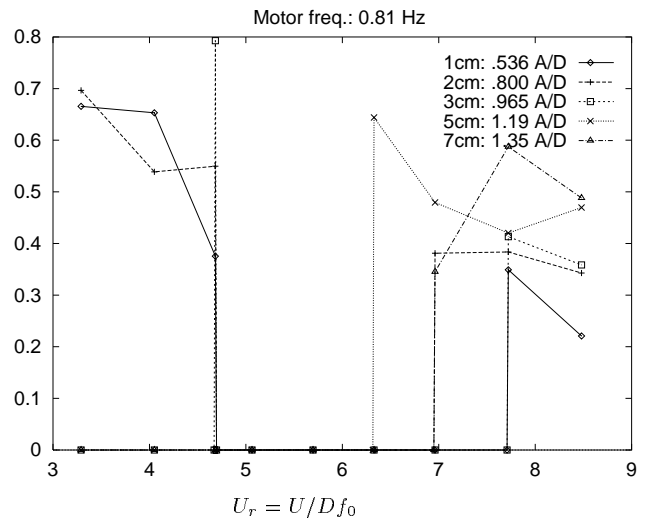


(d) Oscillation amplitude, A/D, at the vortex shedding frequency

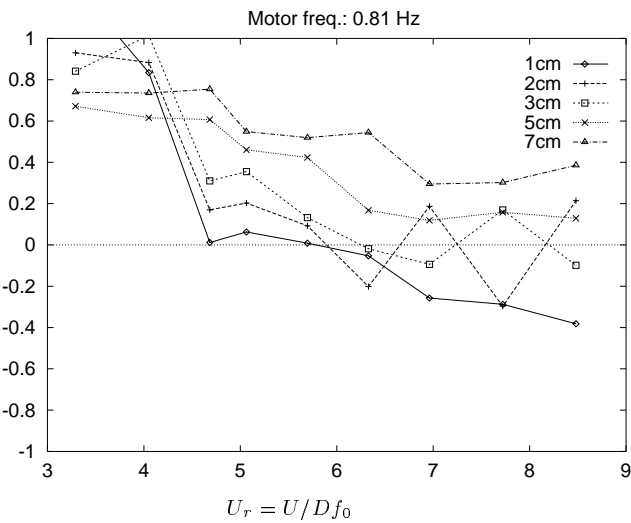
Figure 5: Support excitation at 0.52 Hz



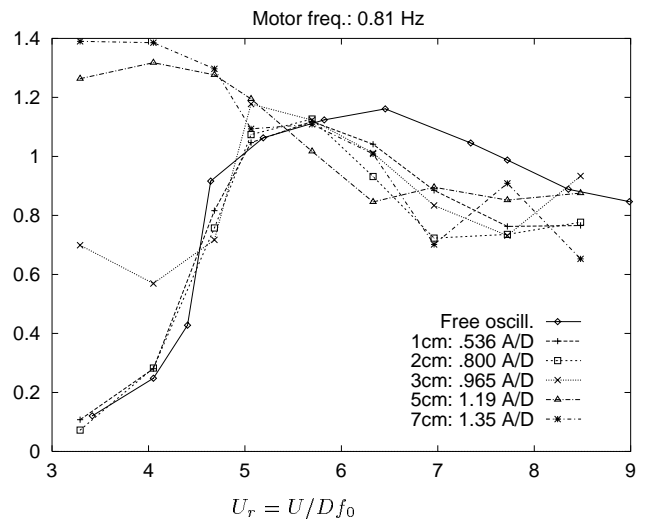
(a) Oscillation frequency due to vortex shedding over support excitation frequency



(b) Oscillation amplitude, A/D, at the support frequency, towed case, over oscillation amplitude in still water. The still water amplitude is found in the legend

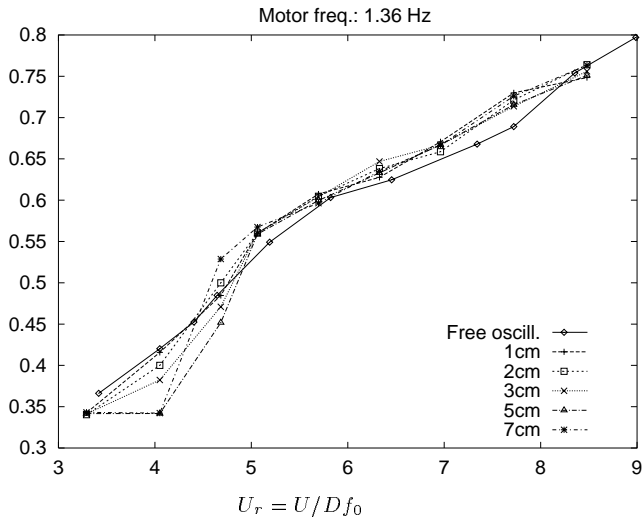


(c) Transverse "Drag coefficient"  $C_d$ : Positive coefficient denotes that the fluid forces take energy away from the system

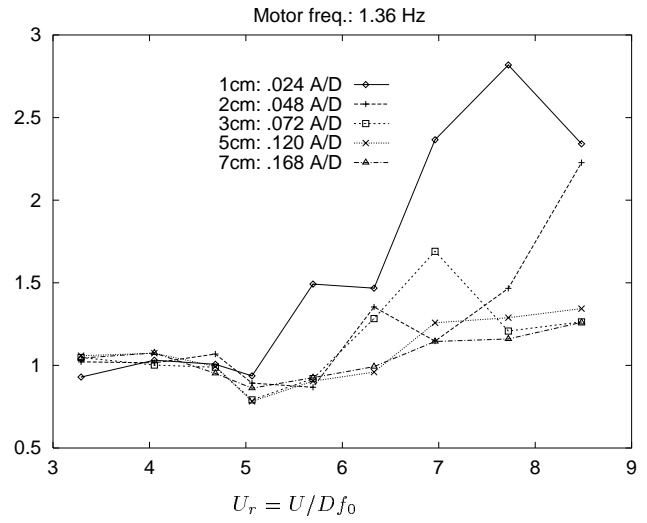


(d) Oscillation amplitude, A/D, at the vortex shedding frequency

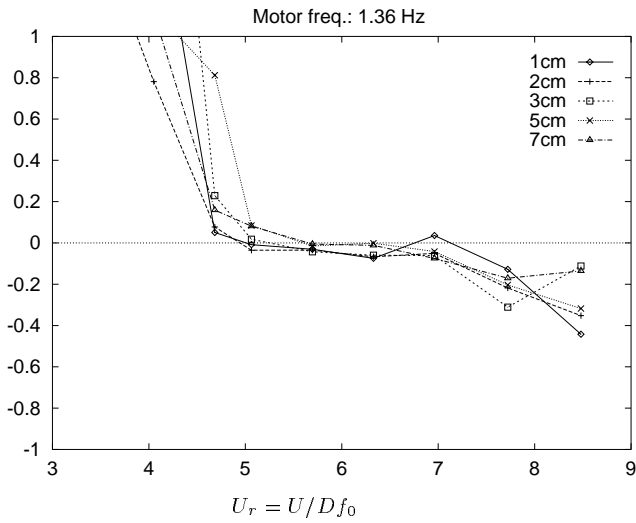
Figure 6: Support excitation at 0.81 Hz



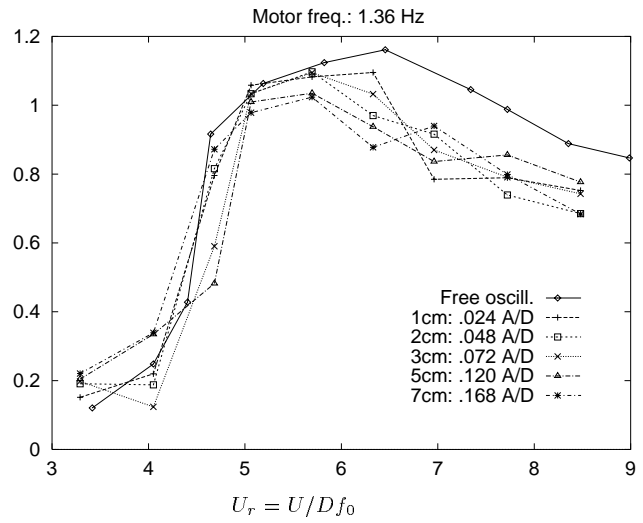
(a) Oscillation frequency due to vortex shedding over support excitation frequency



(b) Oscillation amplitude, A/D, at the support frequency, towed case, over oscillation amplitude in still water. The still water amplitude is found in the legend



(c) Transverse "Drag coefficient"  $C_d$ : Positive coefficient denotes that the fluid forces take energy away from the system



(d) Oscillation amplitude, A/D, at the vortex shedding frequency

Figure 7: Support excitation at 1.36 Hz